Influences of different structures on the characteristics of H_2O-based and O_3-based La_xAl_yO films deposited by atomic layer deposition*

Chen-Xi Fei(费晨曦), Hong-Xia Liu(刘红侠)†, Xing Wang(汪星), Dong-Dong Zhao(赵冬冬), Shu-Long Wang(王树龙), and Shu-Peng Chen(陈树鹏)

Key Laboratory for Wide-Band Gap Semiconductor Materials and Devices of Education, School of Microelectronics, Xidian University, Xi'an 710071, *China*

(Received 5 November 2015; revised manuscript received 14 January 2016; published online 1 April 2016)

H_2O-based and O_3-based La_xAl_yO nanolaminate films were deposited on Si substrates by atomic layer deposition (ALD). Structures and performances of the films were changed by different barrier layers. The effects of different structures on the electrical characteristics and physical properties of the La_xAl_yO films were studied. Chemical bonds in the La_xAl_yO films grown with different structures and different oxidants were also investigated with x-ray photoelectron spectroscopy (XPS). The preliminary testing results indicate that the La_xAl_yO films with different structures and different oxidants show different characteristics, including dielectric constant, equivalent oxide thickness (EOT), electrical properties, and stability.

Keywords: atomic layer deposition, oxidant, dielectric constant, equivalent oxide thickness

PACS: 81.15.Gh, 77.55.D– **DOI:** 10.1088/1674-1056/25/5/058106

1. Introduction

Numerous technological and scientific challenges have to be surmounted to continue Moore's law, which predicts that the device density will double every 18 to 24 months. The aggressive scaling of silicon (Si) electronics that comes along with the scaling of the silicon dioxide (SiO_2) based gate dielectrics leads to unacceptable high gate leakage currents due to direct tunneling.[1,2] With the development of the microelectronics industry, numbers of high-k materials have been investigated as candidates to replace SiO_2 as the gate dielectrics.[3] Candidate materials include Al_2O_3,[4] La_2O_3,[5] HfO_2,[6] and Nd_2O_3,[7] La_2O_3 is an attractive gate dielectric candidate for replacement of SiO_2 in further scaled metal–oxide–semiconductor field effect transistors (MOSFETs) due to several advantages such as a higher permittivity (~ 27), a larger conduction band off-set (~ 2.3 eV), and good thermodynamic stability with Si.[8] However, La_2O_3 is so moisture sensitive that it is considered to be incompatible with large-scale integration processes. La_2O_3 can easily form both La-silicate and La-hydroxide because of the catalytic and hygroscopic behavior. It will cause the decrease of the dielectric constant and the performance degradation of the films.[3] Al_2O_3 has many favorable properties like kinetic stability and thermodynamic stability on Si up to high temperatures, good interface with Si, and low bulk defect density.[9] However, the dielectric constant of Al_2O_3 (6.5–9) is low. Lanthanum aluminate ($LaAlO_3$), which is a compound of La_2O_3 with a high dielectric constant and Al_2O_3 with a large band gap, has high immunity against ambient moisture while offering both comparable thermal stability on Si and high dielectric constant (25–27). Therefore, $LaAlO_3$ is regarded as a promising candidate for high-k gate dielectrics.[10]

Uniform and conformal thin films have a wide variety of applications in semiconductor microelectronics. It is necessary to use a deposition technique that can produce films with good dielectric properties, accurate thickness, and smooth surface.[11] One method that is particularly suitable for making uniform and conformal layers is atomic layer deposition (ALD). ALD is a process for depositing highly uniform and conformal thin films by alternating exposures of a surface to vapors of two chemical reactants. By contrast with metal-organic chemical vapor deposition (MOCVD), molecular beam epitaxy (MBE), and pulsed laser deposition (PLD), ALD is based on self-limiting film growth via alternate saturative surface reaction. Therefore, the films deposited by ALD have high density, high purity, and accurate thickness. In this study, we investigate the La_xAl_yO nanolaminate films with different structures and different oxidants deposited on Si substrates by ALD, which is an attempt to ensure the uniformity and conformity of the films. The electrical characteristics and physical properties of the films with different oxidants (H_2O and O_3) and different structures are studied and compared.

2. Experiment

A P-type Si B-doped (100) wafer with a resistivity of 8–12 Ω·cm was cleaned with a ($HCl : H_2O_2 : H_2O = 1 : 1 : 5$) solution for 10 min at 85 °C to remove organic contamination, and then chemically etched with a diluted hydrofluoric acid solution ($HF : H_2O = 1 : 100$) to remove native oxides, both followed by a 30 s rinse in deionized water. The substrate

*Project supported supported by the National Natural Science Foundation of China (Grant Nos. 61376099 and 61434007).

†Corresponding author. E-mail: hxliu@mail.xidian.edu.cn

© 2016 Chinese Physical Society and IOP Publishing Ltd

was then immediately loaded into the ALD reactor (Picosun R-200, Espoo, Finland). Tris(isopropylcyclopentadienyl) lanthanum [La(^{i}PrCp)$_3$] and trimethylaluminum (TMA) were used as the metal precursor for La_xAl_yO, and H_2O and O_3 served as the oxidants, respectively. Ultra-high purity nitrogen (N_2, 99.999%) was employed as the carrier and purge gas. The container of the aluminum precursor was kept at room temperature, corresponding to a vapor pressure of 10–15 hPa, and the La precursor was kept at 180 °C. The 1.5 nm SiO_2 above the Si substrate (the native oxides had been removed by the diluted hydrofluoric acid solution) was obtained after 0.5 s O_3 pulse/10 s purge with N_2 for 15 min at 300 °C by ALD. The ultra pure O_2 (99.999%) was used in the ozone generator to obtain O_3, the concentration of O_3 was 200 g/Nm^3. La_xAl_yO films were grown on the Si wafers by a layer-by-layer deposition process using different metal processors {TMA and [La(^{i}PrCp)$_3$]} and different oxidants (H_2O and O_3) at 300 °C. The deposition cycles for different kinds of La_xAl_yO laminate profiles are shown in Table 1. When H_2O was used as the oxidant, the ALD sequence was composed of 0.5 s La(^{i}PrCp)$_3$ pulse/6 s purge with N_2/0.5 s H_2O pulse/8 s purge with N_2 and 0.1 s TMA pulse/3 s purge with N_2/0.1 s H_2O pulse/4 s purge with N_2. When O_3 was used as the oxidant, the ALD sequence was composed of 0.5 s La(^{i}PrCp)$_3$ pulse/8 s purge with N_2/0.5 s O_3 pulse/10 s purge with N_2 and 0.1 s TMA pulse/3 s purge with N_2/0.5 s O_3 pulse/4 s purge with N_2. The capacitance–voltage (C–V) measurements were carried out using a Keithley 590 C–V analyzer (Keithley Instruments Inc., Cleveland, OH, USA) at 100 kHz, the diameter of the mercury probe is 859 μmm. The film thicknesses were measured by J. A. Woollam M2000D spectroscopic ellipsometry. The bonding structures of the films were examined by x-ray photoelectron spectroscopy.

Table 1. Samples with different structures and different oxidants.

Sample	Profile and cycles for as-deposited films	Oxidant
A	[(La_2O_3)×3/Al_2O_3]×40	H_2O
B	[(La_2O_3)×3/Al_2O_3]×40+1.5 nm SiO_2	H_2O
C	[(La_2O_3)×3/Al_2O_3]×40+1.5 nm Al_2O_3	H_2O
D	[(La_2O_3)×2/Al_2O_3]×40	O_3
E	[(La_2O_3)×2/Al_2O_3]×40+1.5 nm SiO_2	O_3
F	[(La_2O_3)×2/Al_2O_3]×40+1.5 nm Al_2O_3	O_3

3. Results and discussion

The deposition temperature of ALD should be in the range where the surface-limited reaction occurs with a constant growth rate. Each film has an optimum temperature for the growth. Figure 1 shows the temperature dependence of the La_2O_3 growth rate when the process temperature is varied from 200 °C to 360 °C. The curves with red and blue colors stand for the growth rates of La_2O_3 films when O_3 and H_2O are used as the oxidant, respectively. When H_2O is used as the oxidant, the growth rate of La_2O_3 increases as the temperature increases, and maintains a stable value (0.65–0.7 Å/cycle) when the temperature is above 260 °C. When O_3 is used as the oxidant, the growth rate of La_2O_3 acquires a certain value when the deposition temperature is above 300 °C. A stable growth rate of 1 Å/cycle is obtained in the temperature range of 300–360 °C. Therefore, the temperature ranges of 260–360 °C and 300–360 °C within which the surface-limited reaction would most probably occur are set to investigate the influence of the deposition temperature on the growth rate when H_2O and O_3 are used as the oxidant, respectively.[7] When H_2O and O_3 are used as the oxidant, the growth rates of Al_2O_3 films measured by the spectroscopic ellipsometry are 0.97 Å/cycle and 1.04 Å/cycle, respectively. Therefore, 300 °C is selected as the ALD deposition temperature for La_xAl_yO films. At this temperature, when H_2O and O_3 are used as the oxidant, the growth rates of La_2O_3 films are 0.71 Å/cycle and 1.03 Å/cycle, respectively.

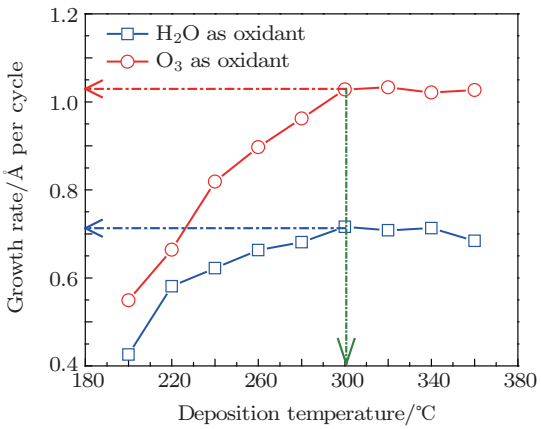


Fig. 1. (color online) Dependence of the La_2O_3 growth rate on the deposition temperature with different oxidants.

Figure 2 shows the C–V characteristics of the La_xAl_yO films with different structures and different oxidants. The gate voltage is swept from negative to positive and then back to negative. In Fig. 2(a), the hysteresis voltage of sample A is 752 mV. The relatively large anticlockwise hysteresis loop during forward and reversed bias sweeps indicates serious charge trapping in the oxide. This could be attributed to the formation of a defective $LaAlSiO_x$, $LaSiO_x$, and $AlSiO_x$ interface layer and Si out diffusion during the ALD process, causing the poor interface quality and large interface state density.[12,13] In contrast, samples B and C possess smaller hysteresis voltages, which are 205 mV and 221 mV, respectively. To a certain extent, in samples B and C, the barrier layers of SiO_2 and Al_2O_3 can retard the interdiffusion of Si, Al, La, and O atoms. The interface layer of sample B is attributed to the formation of $LaAlSiO_x$, $LaSiO_x$, and $AlSiO_x$. The interface layer of sample C is attributed to the formation of $AlSiO_x$. Because of the favorable property of the good interface of the

Al_2O_3 film with silicon, which can reduce the diffusion of La and Si atoms and the formation of La-silicate, compared to sample A, samples B and C possess better interface quality and smaller interface state density. Moreover, the accumulation capacitance increases with the change of the type of the structure; this is attributed to a decrease of the concentration of the interfacial fixed charge and defects.[14] Table 2 shows the physical thickness, flat band voltage (V_{FB}), equivalent oxide thickness (EOT), and dielectric constant of the films. The V_{FB} of samples A and B are −1.37 V and −0.64 V, respectively. This is attributed to the formation of positive fixed charge in the films. The formation of oxygen vacancies in the La_xAl_yO films increases the positive oxide charge due to the growth of a silicate interfacial layer (IL).[15–17] However, V_{FB} of sample C is 0.33 V. The flat band voltage shifts toward the positive direction, which indicates the formation of negative charge in the film. This is attributed to the strong dipole bonding at the interface.[11]

Table 2. Overview of characterization results of samples.

Sample	Physical thickness/nm	V_{FB}/V	EOT/nm	k
A	13.27	–1.37	5.55	9.32
B	15.43	–0.64	3.91	15.39
C	15.19	0.33	3.13	18.90
D	12.85	–0.21	4.76	10.52
E	14.33	0.16	2.94	19.04
F	14.27	1.16	2.67	20.83

In Fig. 2(b), the C–V curves with O_3 as the oxidant show a wide step, which is caused by the trapped holes injected from the La_xAl_yO layer into the depletion layer. The width of the depletion layer in the Si substrate grows with the gate bias increasing. The growth of the depletion layer will stop and the capacitance becomes constant after all the trapped holes in the interface layer are injected into the depletion layer.[6] The hysteresis voltage of sample D is 20 mV, while the hysteresis voltages of samples E and F can be ignored. The negligible hysteresis voltages indicate the good interface quality and small interface state density in samples E and F. Moreover, the accumulation capacitance increases with the change of the type of the structure, this is attributed to a decrease of the concentration of the interfacial fixed charge and defects. Compared to the La_xAl_yO films with H_2O as the oxidant, the films with O_3 as the oxidant possess larger accumulation capacitances, which is attributed to the small EOT and high dielectric constant. According to the previous report,[18] the La_2O_3 film can react with moisture easily and form $La(OH)_3$ which will decrease the whole dielectric constant of the film. The extracted V_{FB} of the La_xAl_yO films in samples D, E, and F are shown in Table 2. The V_{FB} of the three samples are −0.21 V, 0.16 V, and 1.16 V, respectively. These phenomena are attributed to the formation of positive fixed charge because of the formation of oxygen vacancies in sample D. The increase of the positive oxide charge is due to the interdiffusion of Si, Al, La, and O atoms, and the growth of the silicate interfacial layer is attributed to the formation of $LaSiO_x$, $AlSiO_x$, and $LaAlSiO_x$.[19] Compared to the La_xAl_yO films with H_2O as the oxidant, the films with O_3 as the oxidant possess smaller V_{FB}. This indicates that the La_xAl_yO films with O_3 as the oxidant have smaller EOT and better quality interfacial layers.

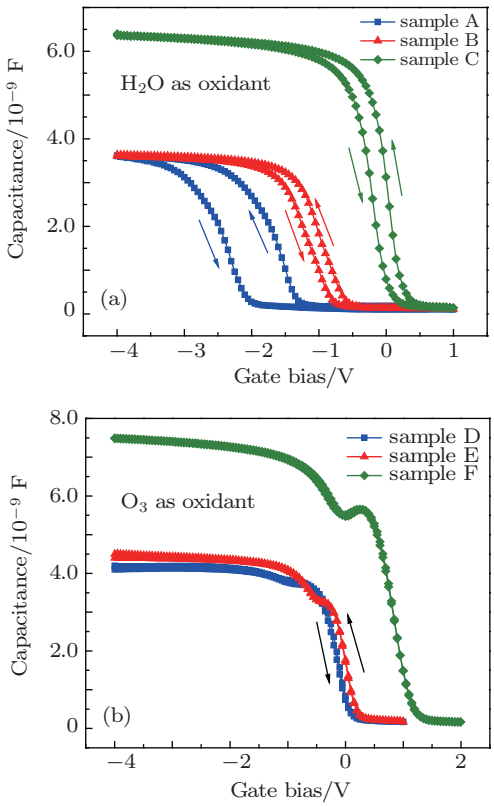


Fig. 2. (color online) The C–V characteristics of La_xAl_yO films deposited with different oxidants: (a) H_2O, (b) O_3.

The EOT and permittivity are determined as follows:

$$\mathrm{EOT} = A\frac{\varepsilon_0\varepsilon_{SiO_2}}{C_{ox}}, \tag{1}$$

$$\mathrm{EOT}_{high-k} = \mathrm{EOT} - T_{SiO_x}, \tag{2}$$

$$\varepsilon_{high-k} = \frac{T_{high-k}}{\mathrm{EOT}_{high-k}}\varepsilon_{SiO_2}, \tag{3}$$

where A is the area, C_{ox} is the accumulation capacitance of the films, T_{SiO_2} and T_{high-k} are the thicknesses of the native oxide and the deposited films, ε_{high-k} is the permittivity of the La_xAl_yO films, and ε_0 and ε_{SiO_2} are the permittivities of vacuum and SiO_2, respectively.

In Table 2, for the same structure, the physical thicknesses of samples A, B, and C are larger than those of samples D, E, and F. This is attributed to the formation of a thicker IL in the samples that H_2O is used as the oxidant. The extracted dielectric constant and EOT of the samples are shown in Fig. 3. In Fig. 3(a), the EOT decreases and the dielectric constant increases by varying the type of the structure of the

films. For sample A, the large EOT is attributed to the formation of $LaSiO_x$, $LaAlSiO_x$, and $AlSiO_x$ which is due to the interdiffusion of La, Al, O atoms from La_2O_3 and Al_2O_3 films close to the substrate and Si atoms from the Si substrate. On the other hand, the small dielectric constant is attributed to the formation of $La(OH)_3$, which is mainly due to a moisture adsorption at the top surface of La_2O_3. For sample B, the EOT and the dielectric constant are 3.91 nm and 15.39, respectively. Similar to sample A, sample B has an interface layer of $LaSiO_x$, $LaAlSiO_x$, and $AlSiO_x$.[20] However, because of the existence of the SiO_2 layer, the interdiffusion of La, Al, O, and Si atoms are restrained. The formation of $LaSiO_x$, $LaAlSiO_x$, and $AlSiO_x$ is mainly due to the interdiffusion of La, Al, and O atoms and Si atoms from the SiO_2 barrier layer. This leads to a smaller interface layer in sample B. Furthermore, for sample C, the EOT and the dielectric constant are 3.13 nm and 18.90, respectively. The smallest EOT is attributed to the Al_2O_3 layer which possesses a good interface with silicon and can restrain the diffusion of La and Al atoms into the Si substrate. Only a few $AlSiO_x$ are formed between the Al_2O_3 layer and the Si substrate.

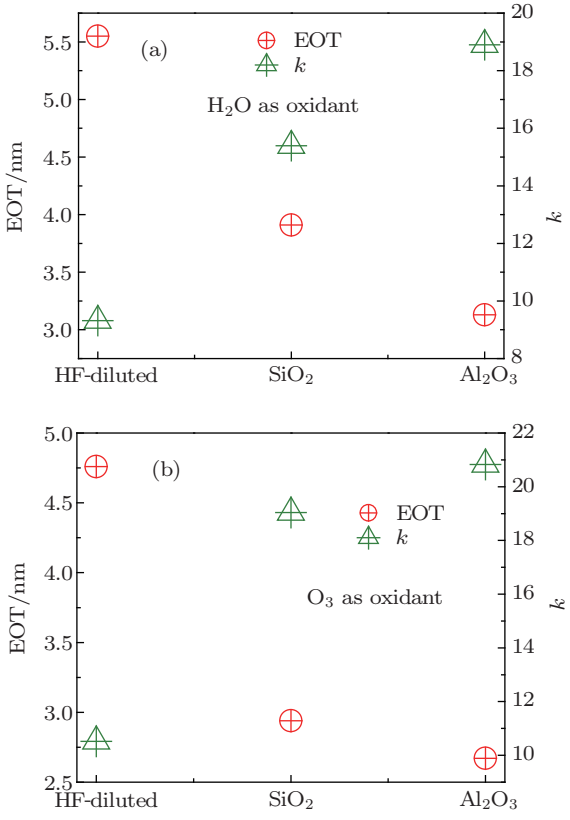


Fig. 3. (color online) Dielectric constant and EOT of La_xAl_yO films deposited with different oxidants: (a) H_2O, (b) O_3.

The EOT and the dielectric constants of samples D, E, and F are 4.76 nm, 2.94 nm, 2.67 nm and 10.52, 19.04, 20.83, respectively, as shown in Fig. 3(b). For the same structure, the dielectric constants of the films with H_2O as the oxidant are lower than those with O_3 as the oxidant. This phenomenon is mainly attributed to the more La-hydroxide and La-silicate formed during the ALD process. The La_2O_3 films react with moisture from the H_2O oxidant, carrier and purge gas and form $La(OH)_3$. Moreover, the La-silicate also decreases the dielectric constants of the films. For the films with O_3 as the oxidant, moisture only comes from the carrier, purge gas and less La-hydroxide is formed in the films. This explains why the films possess relative higher dielectric constants. However, the dielectric constants we obtained are smaller than the theoretical ones of the $LaAlO_3$ films, this probably is due to the fact that the La_xAl_yO films are preserved in air for a long time after deposition, which prohibit the La_2O_3 films from reacting to moisture in air and forming La-hydroxide.

In order to confirm the above analyses, XPS spectra were obtained with using Al $K\alpha$. The binding energy (BE) was calibrated with the position of the C 1s peak at 284.8 eV. Figure 4 depicts the XPS Al 2p, La $3d_{5/2}$, O 1s, and Si 2p spectra of the La_xAl_yO films with H_2O as the oxidant. As shown in Fig. 4(a), the Al 2p spectrum is fitted with three peaks after the application of a smart background. Blue and green curves stand for the Al–O–La and Al–O–Al peaks, respectively.[21] The existence of Al–O–La and Al–O–Al bonds is attributed to the formation of La_xAl_yO and Al_2O_3 in the films. The red curves stand for the aluminium compound formed in the films. The binding energy of aluminates in sample C is slightly higher than that in samples A and B; this indicates that the types of aluminium compound are different between sample C and the other two samples.[6] Sample A contains Al–O–Si and Al–La–O–Si bonds, which are attributed to the diffusion of La and Al atoms into the Si substrate. Similar to sample A, sample B also contains the Al–O–Si and Al–La–O–Si bonds. However, the Si atoms in these bonds come from the SiO_2 barrier layer, while the Al–O–Si bonds in sample C are attributed to the reaction of the Al_2O_3 barrier layer with the Si substrate. On the other hand, the intensity of the Al–O–La peak of sample A is smaller than that of sample B; the intensity of aluminium compound peak of sample A is larger than that of sample B. Thus, sample B possesses a smaller EOT and a higher k than sample A. The O 1s spectra of samples A and B are fitted with three peaks after the application of a smart background, as shown in Fig. 4(b). Red, green, and blue curves stand for the La–O–La, La–O–Al, and La–Al–O–Si contributions, respectively.[12,20,22] The La–O–La bonds are attributed to the formation of La_2O_3 in the films during the ALD process. The pink curve of sample C stands for the Al–O–Al bonds of the Al_2O_3 barrier layer. The binding energy of the peak indicated by the blue curve for sample C is slightly higher than that for samples A and B; this indicates that the types of chemical compound in the IL are different between sample C and the other two samples. The XPS analyses of O 1s are in consonance with the analyses of Al 2p. Figure 4(c) shows the La $3d_{5/2}$ spectra of the samples. The La–Al–O, La–O–La, silicates, and

La–OH bonds are indicated by green, blue, red, and brown curves, respectively.[12,23] The existence of La–OH peaks is attributed to the formation of $La(OH)_3$ which is mainly due to the moisture adsorption of La_2O_3. The variation tendency of La–O–Al and silicates bonds of samples A and B in the La $3d_{5/2}$ XPS spectrum is in accordance with that in the Al 2p and O 1s XPS spectra. Figure 4(d) shows the Si 2p spectra of the samples. The binding energy located at 99.3 eV is the Si^0 peak, which is attributed to the Si substrate.[24] The higher peaks indicated by black are satellite peaks. The green and red curves indicate Si^{3+} and Si^*+Si^{4+}, respectively, which come from the silicates and SiO_{2-x}.[22,24] The shift of the peaks of the silicates indicates that the types of chemical bonds of silicates are different. For sample B, because of the existence of the SiO_2 barrier layer, the amount of silicates in the sample is smaller than that in sample A. This causes the smaller EOT of sample B. On the other hand, the existence of Si^*+Si^{4+} is attributed to the formation of SiO_2 between the Si substrate and the Al_2O_3 barrier layer.

Figures 5(a)–5(d) show the XPS Al 2p, La $3d_{5/2}$, O 1s, and Si 2p spectra of the $LaAlO_3$ films with O_3 as the oxidant, respectively. The variation trends of the chemical bonds of Al 2p and O 1s of the films are similar to those of the films with H_2O as the oxidant. However, in the La $3d_{5/2}$ spectra, the La–OH bonds are observed as shown in Fig. 5(c). The formation of La–OH bonds may be due to the reaction of moisture from air with La_2O_3 at the top of the $LaAlO_3$ layer. The existence of La-hydroxide decreases the dielectric constants of the films. The intensity of Si^*+Si^{4+} in the Si 2p spectrum decreases with the change of the type of the sample, and the film with Al_2O_3 barrier possesses smaller IL and EOT. All the XPS analyses are in accord with the analyses of electrical characteristics of the films discussed previously.

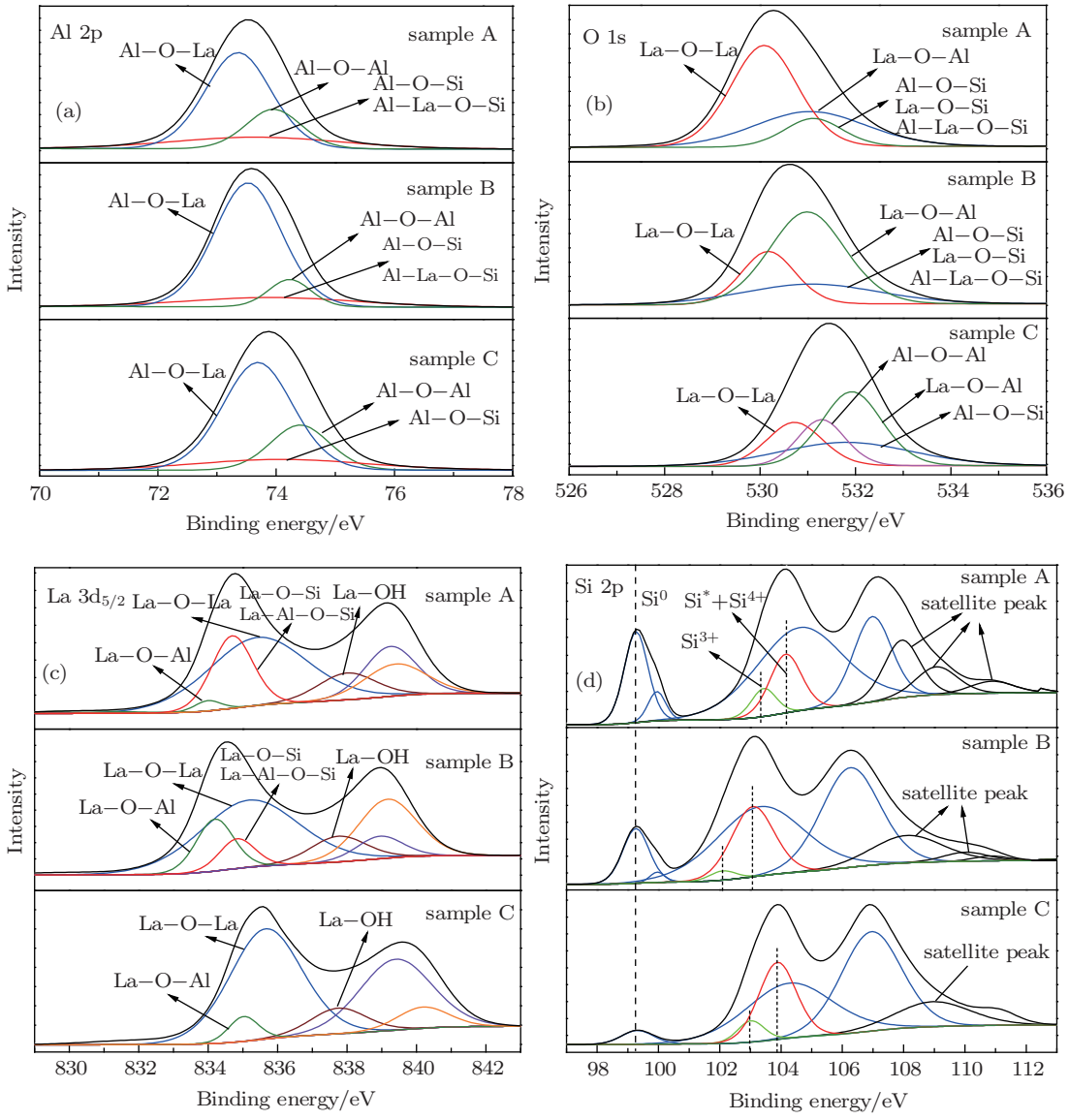


Fig. 4. (color online) XPS spectra of the La_xAl_yO nanolaminates with H_2O as the oxidant: (a) Al 2p, (b) O 1s, (c) La $3d_{5/2}$, (d) Si 2p.

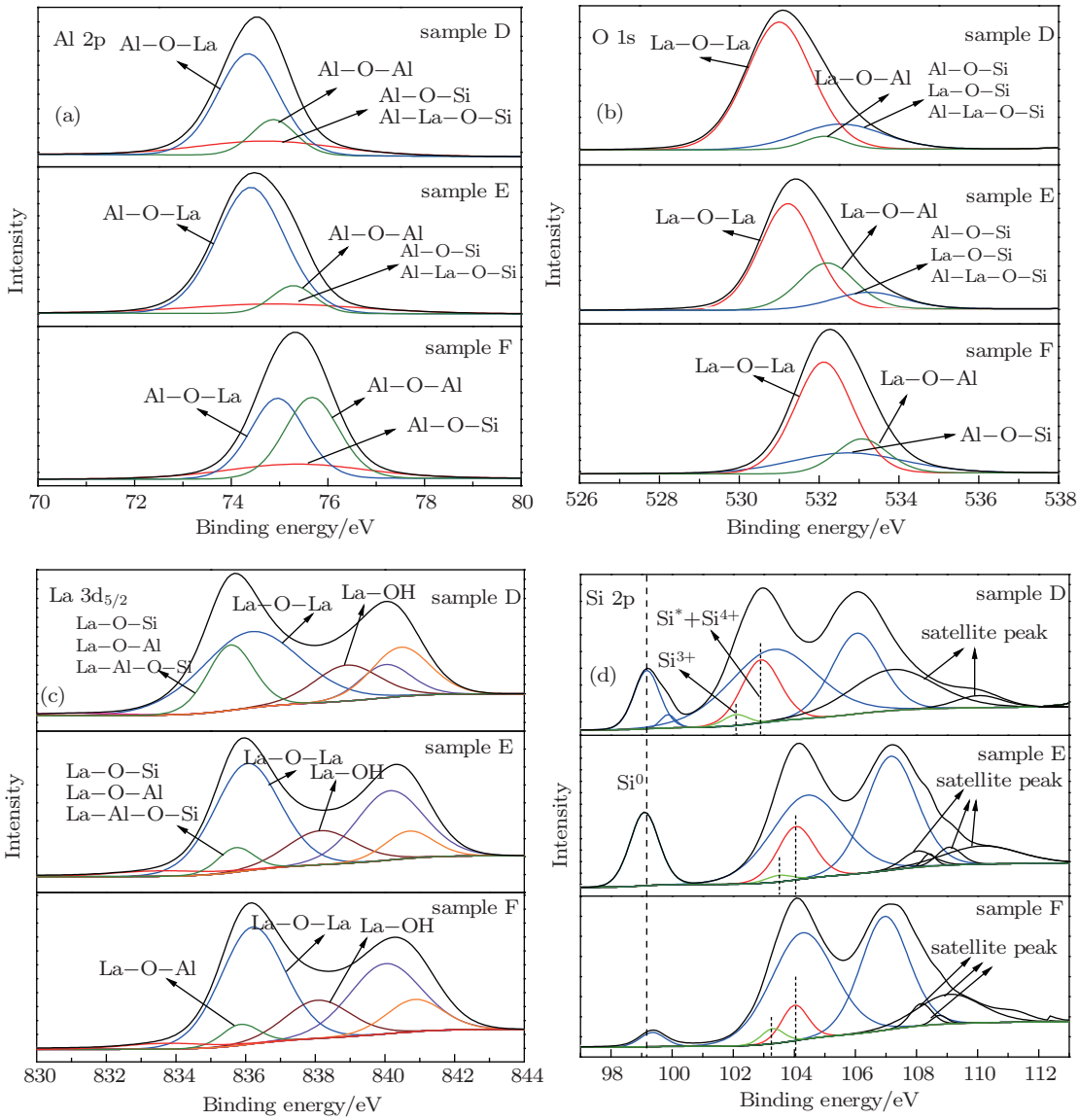


Fig. 5. (color online) XPS spectra of the La_xAl_yO nanolaminates with O_3 as the oxidant: (a) Al 2p, (b) O 1s, (c) La $3d_{5/2}$, (d) Si 2p.

4. Conclusion

In this study, La_xAl_yO nanolaminate films with different structures and different oxidants were deposited on Si substrates by ALD. The La_xAl_yO films with H_2O and O_3 used as the oxidants and a barrier layer of Al_2O_3 possessed the highest dielectric constants (18.90 and 20.83) and the smallest EOT (3.13 and 2.67) among the films studied. Moreover, compared to the H_2O-based La_xAl_yO films, the O_3-based films were superior in dielectric constant, EOT, and hysteresis voltage. Furthermore, due to the kinetic and thermodynamic stability on Si, the Al_2O_3 barrier layer can restrain the interdiffusion of La, O, and Si atoms and make films possess superior performances.

References

[1] Cao D, Cheng X, Yu Y, Li X, Liu C, Shen D and Mändl S 2013 *Appl. Phys. Lett.* **103** 081607

[2] Zheng L, Cheng X, Cao D, Wang Z, Xia C, Yu Y and Shen D 2014 *Appl. Phys. Lett.* **104** 023112

[3] Flege J I, Kaemena B, Höcker J, Bertram F, Wollschläger J, Schmidt T and Falta J 2014 *Appl. Phys. Lett.* **104** 131604

[4] Zhang X, Liu B W, Zhao Y, Li C B and Xia Y 2013 *Chin. Phys. B* **22** 127303

[5] Park T J, Sivasubramani P, Coss B E, Kim H C, Lee B, Wallace R M, Kim J, Rousseau M, Liu X, Li H, Lehn J S, Hong D and Shenai D 2010 *Appl. Phys. Lett.* **97** 092904

[6] Fan J B, Liu H X, Gao B, Zhuo Q Q and Hao Y 2012 *Chin. Phys. B* **21** 087702

[7] Fan X J, Liu H X and Zhang X J 2013 *Appl. Phys. A* **114** 545

[8] Zhang X, Tu H, Zhao H, Yang M, Wang X, Xiong Y, Yang Z, Du J, Wang W and Chen D 2011 *Appl. Phys. Lett.* **99** 132902

[9] Park D W, Mikael S, Chang T H, Gong S and Ma Z 2015 *Appl. Phys. Lett.* **106** 102106

[10] Suzuki M, Yamaguchi T, Fukushima N and Koyama M 2008 *J. Appl. Phys.* **103** 034118

[11] Qiu H B, Li H Q, Liu B W, Zhang X and Shen Z N 2014 *Chin. Phys. B* **23** 027301

[12] Maeng W J, Kim W H and Kim H 2010 *J. Appl. Phys.* **107** 074109

[13] Kundu S, Maurya D, Clavel M, Zhou Y, Halder N N, Hudait M K, Banerji P and Priya S 2014 *Sci. Rep.* **5** 8494

[14] Liu W J, Liao M Y, Imura M, Oosato H, Watanabe E and Koide Y 2013 *Appl. Phys. Lett.* **102** 112910
[15] Molina J, Tachi K, Kakushima K, Ahmet P, Tsutsui K, Sugii N, Hattori T and Iwai H 2007 *J. Electrochem. Soc.* **154** G110
[16] Suzuki M 2012 *Materials* **5** 443
[17] Lee B, Novak S R, Lichtenwalner D J, Yang X and Misra V 2011 *IEEE Trans. Electron. Dev.* **58** 3106
[18] Lamagna L, Wiemer C, Perego M, Volkos S N, Baldovino S, Tsoutsou D, Schamm-Chardon S, Coulon P E and Fanciulli M 2010 *J. Appl. Phys.* **108** 084108
[19] Li X L, Xiang W F, Lu H B and Ma Z H 2005 *J. Appl. Phys.* **97** 124104
[20] Cao D, Cheng X, Jia T, Xu D, Wang Z, Xia C, Yu Y and Shen D 2013 *J. Vac. Sci. Technol. B.* **31** 01A113
[21] Liu J W, Liao M Y, Imura M, Oosato H, Watanabe E, Tanaka A, Iwai H and Koide Y 2013 *J. Appl. Phys.* **114** 084108
[22] Das T, Mahata C, Maiti C K, Dalapati G K, Chia C K, Chi D Z, Chiam S Y, Seng H L, Tan C C, Hui H K, Sutradhar G and Bose P K 2012 *J. Electrochem. Soc.* **159** G15
[23] Ma J W, Lee W J, Cho M H, Lee K M, Sohn H C, Kim C S and Cho H J 2011 *J. Appl. Phys.* **109** 124106
[24] Ma J W, Lee W J, Cho M H, Chung K B, An C H, Kim H, Cho Y J, Moon D W and Cho H J 2011 *J. Electrochem. Soc.* **158** G79